

# U-Pb zircon geochronology of basaltic pyroclastic rocks from the basement beneath the Xisha Islands in the northwestern South China Sea and its geological significance

Yu Zhang<sup>1, 2, 3</sup>, Kefu Yu<sup>1, 2, 3\*</sup>, Shiyong Li<sup>4</sup>

<sup>1</sup> Guangxi Laboratory on the Study of Coral Reefs in the South China Sea, Guangxi University, Nanning 530004, China

<sup>2</sup> Coral Reef Research Center of China, Guangxi University, Nanning 530004, China

<sup>3</sup> School of Marine Sciences, Guangxi University, Nanning 530004, China

<sup>4</sup> Key Laboratory of Ocean and Marginal Sea Geology, South China Sea Institute of Oceanology, Chinese Academy of Science, Guangzhou 510301, China

Received 17 November 2022; accepted 27 March 2023

© Chinese Society for Oceanography and Springer-Verlag GmbH Germany, part of Springer Nature 2024

## Abstract

As one of the micro-blocks dispersed in the South China Sea (SCS), the basement of the Xisha Islands has rarely been drilled because of the thick overlying Cenozoic sediments, which has led to a confused understanding of the pre-Cenozoic basement of the Xisha Islands. Well CK-1, a kilometer-scale major scientific drill in the Xisha Islands in the northwestern SCS, penetrated thick reefal limestone (0–888.4 m) and the underlying basement rocks (888.4–901.4 m). In this study, we present the zircon U-Pb ages of basement basaltic pyroclastic rocks from Well CK-1 in the Xisha Islands of the northwestern SCS to investigate the basement nature of the Xisha micro-block. The basement of Well CK-1 consists of basaltic pyroclastic rocks on the seamount. The zircon grains yielded apparent ages ranging from ca. 2138.9 Ma to ca. 36 Ma. The old group of zircon grains from Well CK-1 was considered to be inherited zircons. Two Cenozoic zircons gave a weighted mean  $^{206}\text{Pb}/^{238}\text{U}$  age of  $(36.3 \pm 1.1)$  Ma, Mean Squared Weighted Deviations (MSWD) = 1.2, which may represent the maximum age of the volcano eruption. The Yanshanian inherited zircons (116.9–105.7 Ma and 146.1–130.2 Ma) from Well CK-1 are consistent with the zircons from Well XK-1, indicating that the basement of Chenhang Island may be similar to that of Well XK-1. We propose that the Xisha micro-block may have developed on a uniform Late Jurassic metamorphic crystalline basement, intruded by Cretaceous granitic magma.

**Key words:** South China Sea, Xisha Islands, basaltic pyroclastic rocks, zircon

**Citation:** Zhang Yu, Yu Kefu, Li Shiyong. 2024. U-Pb zircon geochronology of basaltic pyroclastic rocks from the basement beneath the Xisha Islands in the northwestern South China Sea and its geological significance. *Acta Oceanologica Sinica*, 43(2): 83–93, doi: 10.1007/s13131-023-2198-2

## 1 Introduction

Knowledge of the basin basement provides important evidence for the inversion of the basin's tectonic evolution and is an important part of basic geological research on the basin. Studying on the composition and properties of the basement can provide an important theoretical basis for discussing the relationship between adjacent plates, tectonic characteristics, formation mechanisms, and the tectonic evolution of adjacent areas (Xu et al., 2007; Zhang et al., 2007; Guynn et al., 2012; Zhao and Zhai et al., 2013; Xie et al., 2014; Tang et al., 2017). Furthermore, the basement is the material basis for the formation and evolution of sedimentary basins and is also related to the formation of overlying basins and their hydrocarbon-bearing properties. The basement controls the sedimentary pattern and genetic mechanism of the basin and the type and distribution of hydrocarbon traps in the sedimentary basins (Chen et al., 2005; Liu et al., 2004a, 2004b, 2011; Deng et al., 2005; Gao et al., 2007; Li et al., 2012; Mora-Bohórquez et al., 2017; He et al., 2017). Therefore, scientific re-

search on basin basements is not only helpful for studying the formation of sedimentary basins but also has important guiding significance for studying the tectonic evolution process of adjacent plates.

The South China Sea (SCS) is one of the largest marginal sea basins of Eastern Asia, which is located at the junction of the Pacific Plate, the Eurasian Plate, and the Indo-Australian Plate (Lin et al., 2009; Guo et al., 2016a; Sun, 2016; Zhang et al., 2018, 2020a, 2020b; Miao et al., 2021). Although the SCS basin is small and young, the SCS has almost experienced a complete Wilson cycle (Li et al., 2013; Fang et al., 2017; Wang et al., 2016; Yang and Fang, 2015; Zhang et al., 2020b). Therefore, the SCS is considered as a natural laboratory for the study of many lithospheric processes such as continental break-up, ocean basin expansion, and subduction (Li et al., 2013, 2015; Yan et al., 2008c, 2010).

Because of the thick Cenozoic sediments overlying the continental basement in the northern SCS, the continental basement has rarely been drilled. As a result, there is a confused un-

Foundation item: The National Natural Science Foundation of China under contract Nos 42030502, 42090041 and 42166003, the Guangxi Scientific Projects under contract Nos AD17129063 and AA17204074, the Guangxi Youth Science Fund Project under contract 2019GXNSFBA185016; the Ph.D. Research Start-up Foundation of Guangxi University under contract No. XBZ170339.

\*Corresponding author, E-mail: [kefuyu@scsio.ac.cn](mailto:kefuyu@scsio.ac.cn)

derstanding of the pre-Cenozoic continental basement of the northern SCS (Liu et al., 2004a, 2011; Lu et al., 2011; Sun et al., 2014; Xiu et al., 2016; Zhu et al., 2017). The International Ocean Discovery Program Expedition (IODP) 367/368 expeditions suggest that the basement of the Liwan sub-basin consists of fore arc-inherited anisotropic meta-sediments (Zhang et al., 2020c). Some scholars have identified a Precambrian metamorphic crystalline basement in the northern SCS based on geophysical data (Compiled by the Second Marine Geological Investigation Brigade of the Ministry of Geology and Mineral Resources, 1987; Liu and Zhan, 1994; Yao and Wan, 2006; Hao et al., 2009; Lu et al., 2011; Sun et al., 2014). Previous researchers have obtained gneiss from the Pearl (Zhujiang) River Mouth Basin of the northern SCS; however, high-precision dating data are still lacking. At present, it is uncertain whether gneiss is the product of a Precambrian crystalline basement or late tectonic metamorphism (Sun et al., 2014).

Well XY-1, located on Yongxing Island, was the first well to penetrate reef limestone and reach the metamorphic crystalline basement of the Xisha Islands. The basement rocks are mainly composed of granitic gneiss and biotite plagioclase gneiss with an Rb-Sr age of 627 Ma (Wang et al., 1979). Based on the Rb-Sr age of Well XY-1 (627 Ma), some researchers have proposed that the northwestern region of the SCS developed on top of a Precambrian crystalline block (Liu and Zhan, 1994; Liu et al., 2004a, 2011; Yue et al., 2013; Sun et al., 2014).

The age of the metamorphic rocks in Well XY-1, as determined by bulk Rb-Sr analysis, is likely to have no specific geological significance (Zhu et al., 2017). According to the data from Well XY-1, both orthometamorphites and parametamorphites were present (Sun, 1987). The analyzed sample from Well XY-1 may not have been a typical orthometamorphite. The resulting Rb-Sr isochron line was derived from multiple samples that generated older ages (Sun, 1987). Sun (1987) redated the basement rocks of Well XY-1 and obtained the K-Ar age of  $(96.341 \pm 1.18)$  Ma, which represents the age of the last metamorphic event, and proposed that the Xisha basement formed between 627 Ma and 96 Ma (Sun, 1987). Well XK-1, located 1 km from XY-1, is another deep well that penetrates the reef limestone. Zircon U-Pb dating indicates that the basement rocks are Late Jurassic plagiogneisses [ $(152.9 \pm 1.7)$  Ma], which were intruded by Early Cretaceous granitic magma [ $(107.8 \pm 3.6)$  Ma] (Zhu et al., 2017).

Whether the northern SCS developed on top of a uniform Precambrian metamorphic crystalline basement remain controversial. In this study, we present the LA-ICP-MS zircon U-Pb ages of basaltic pyroclastic rocks from Well CK-1, Chenhang Island, Xisha Islands, SCS, to determine the time of magmatic activity. In addition, a comparison of magmatic activity in the SCS and surrounding areas enabled us to identify the basement nature of the Xisha Reef Islands.

## 2 Geological setting and sample description

According to bathymetric, gravity, and magnetic maps, the SCS basin can be divided into three sub-basins: Northwest sub-basin, East sub-basin, and Southwest sub-basin. Based on a seafloor magnetic survey, the East sub-basin is the largest sub-basin formed by north-south extension (Briaies et al., 1993; Taylor and Hayes, 1982). More recently, constrained by an investigation of the IODP 349, the onset of seafloor spreading began at 33 Ma. Seafloor spreading stopped at approximately 15 Ma in the East sub-basin, and about 16 Ma in the Southwest subbasin (Li et al., 2014, 2015). A southward-spreading ridge jump occurred around 23.6 Ma in the East sub-basin (Li et al., 2014).

Several micro-blocks are dispersed within the SCS, including the Xisha, Zhongsha, Dongsha, Nansha, and Reed-Northeastern Palawan blocks (Li et al., 2013; Liu et al., 2004a, 2011; Yao et al., 2004; Zhang et al., 2018, 2020b; Yan et al., 2008b, 2010, 2014, 2015). Previous studies have suggested that the continental basement is widely distributed across all micro-blocks (Yan et al., 2010 and references therein). These micro-blocks were considered as a whole in a large micro-block during Paleo-Tethys times, which was named the “Qiongdongnan block” (Liu et al., 2002, 2006). These blocks began to separate from each other because of thinning and extension of the SCS lithosphere during the Late Cretaceous (Liu et al., 1999; Yao et al., 2004; Xiu et al., 2016). The Xisha micro-block, located in the northwest part of the northern continental slope of the SCS, is bounded by the Qiongdongnan Basin in the northwest, the Xisha Trough in the north, and the Dongsha Trough in the east. It is a thinned continental crust, and its basement may have been affected by multi-stage magmatism (Qiu et al., 2006; Huang et al., 2011a, 2011b; Guo et al., 2016b; Xiu et al., 2016).

Well CK-1 which is located just 20 m from Well CK-2, was drilled on Chenhang Island of Xisha Islands from an altitude of +1.0 m to a bottom depth of 904.14 m (Fig. 1). The Well penetrated thick reefal limestone (0–888.4 m) and underlying basement rocks (888.4–901.4 m). The basement of Well CK-1 consisted of basaltic pyroclastic rocks. The basaltic pyroclastic rocks are gray-green in color. They were extensively weathered and exhibited the vesicular and amygdaloidal structures under a microscope. The amygdalae were mainly oval and round in shape, with a few irregular ones in some parts, and the filling minerals were mainly calcite, opal, chalcedony, and zeolite. The main crystalline clastic mineral was clinopyroxene, with a small amount of plagioclase (Fig. 2). The crystal clastics are usually subangular or angular in shape, indicating that the basaltic pyroclastic rocks are in situ or nearby volcanism. In addition, there were a few marine fossils in the basaltic pyroclastic rocks. Li et al. (2019) studied the mineral chemistry of clinopyroxene in basaltic pyroclastic rocks in Well CK-1. The clinopyroxenes are mainly composed of diopside, which have high  $\text{Al}_2\text{O}_3$  (5.54%–10.20%), CaO (21.88%–22.62%) and low  $\text{SiO}_2$  (41.40%–48.44%) contents and high  $\text{Al}^{\text{IV}}$ , indicating that parental magma of the basaltic pyroclastic rocks belongs to a silica-undersaturated alkaline series. The Ca, Fe, and Ti concentrations increased from the core to the rim, indicating that the evolution trend of the host magma of pyroxene coincided with that of the alkali rock series. Clinopyroxene discrimination diagrams show that the parental magma formed in an intraplate tectonic setting (Li et al., 2019). LA-ICP-MS analysis of clinopyroxenes in basaltic pyroclastic rocks from Well CK-2 suggested that the parental magma was characterized by high temperature, low pressure, and low oxygen fugacity (Zhang et al., 2018). We collected a 3 kg basaltic pyroclastic rock sample from Well CK-1. The selected samples were weakly weathered.

## 3 Analytical methods

Zircon grains were using conventional heavy liquid and magnetic methods at Langfang Geoscience Exploration Technology Services Co., Ltd., Hebei Province, China. The zircon grains were mounted on epoxy resin discs that were ground and polished to a half-section, exposing the cores of the zircon grains.

Zircon cathodoluminescence (CL) images were obtained at the Langfang Geoscience Exploration Technology Services Co., Ltd., Hebei Province, China, to observe the internal textures of the crystals and select potential target sites. Zircon U-Pb dating and trace element analyses were analyzed using an Agilent 7 900 ICP-MS, coupled with a Resonetics RESolution S-155 ArF 193-

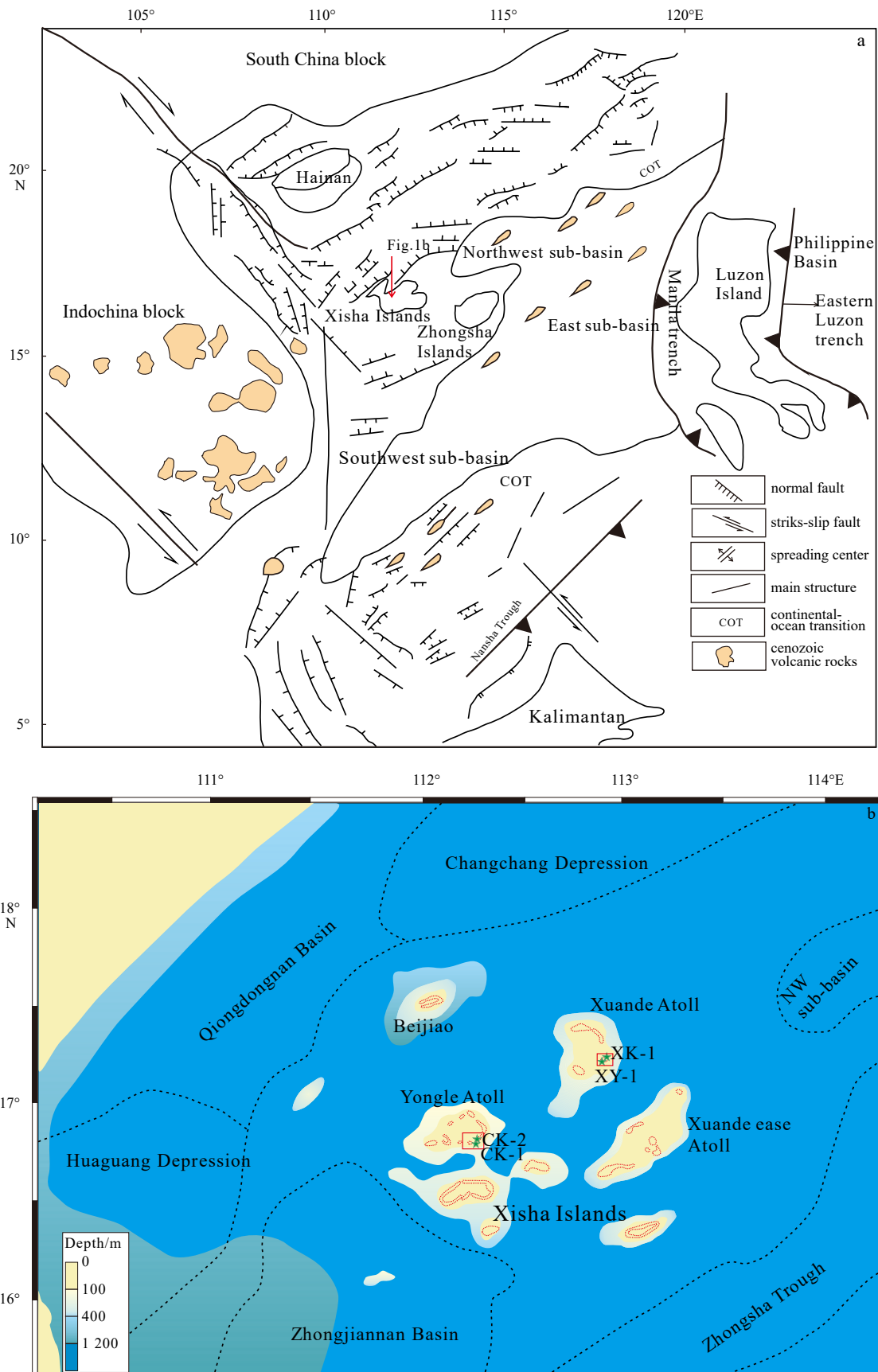


**Fig. 1.** Geological sketch of the SCS and its adjacent areas (a); location of Well CK-1 (b) (Zhang et al., 2018; Wang et al., 2018). The depth is below sea level and in meters.

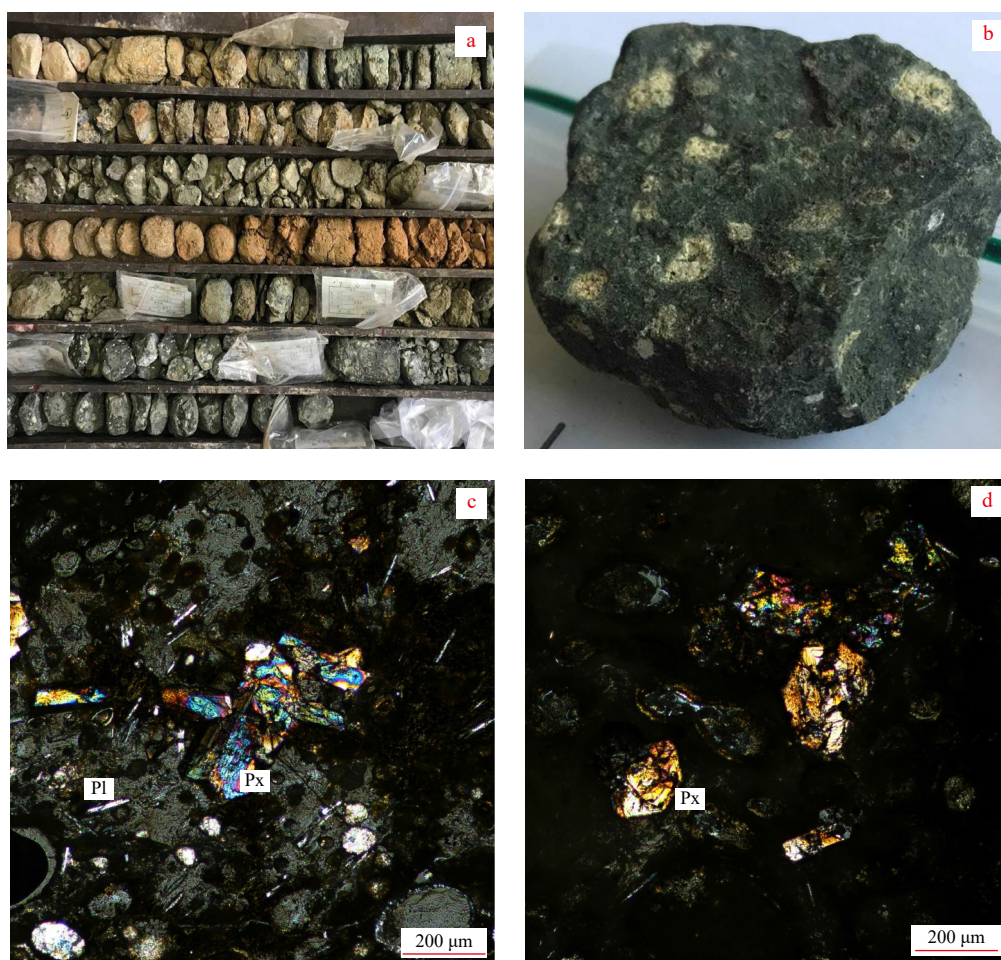


**Fig. 2.** Photographs of the basaltic pyroclastic rocks in hand specimen and under the microscope (cross polarized). Labels represent: Px-pyroxene; Pl: plagioclase.

nm laser ablation system (spot size of 29  $\mu\text{m}$ , repetition frequency of 8 Hz, and ablation time of 40 s). Harvard 91 500 zircon (age = 1 064 Ma; [Wiedenbeck et al., 1995](#)) was used as an external standard for age calculations, and NIST SRM 610 glass was used as an external standard for U, Th, and Pb concentration calculations. Calculations of the zircon isotope ratios and zircon trace elements were performed using the ICPMS DataCal program ([Liu et al., 2008, 2010](#)). Concordia diagrams were constructed using ISOPLOT 3.23 V ([Ludwig, 2003](#)).

#### 4 Analytical results

Total of twenty-five spots were analyzed on twenty-two zircon grains selected from the basaltic pyroclastic rock sample during this study. The LA-ICP-MS dating results are listed in [Table 1](#). CL images of representative zircons are shown in [Fig. 3](#). The zircon grains are generally euhedral and subhedral and 50–150  $\mu\text{m}$  in length, with length-to-width ratios of 1:3. Oscillatory or blurry zoning was observed in CL images ([Fig. 3](#)). The zircon grains have variable Th ( $35 \times 10^{-6}$ – $760 \times 10^{-6}$ ) and U ( $49 \times 10^{-6}$ – $568 \times 10^{-6}$ ) concentrations, yielding Th/U ratios of 0.42–1.62 ([Table 1](#)), suggesting magmatic origins ([Hanchar and Hoskin, 2003](#)).

Most of the analysis points were plotted on or near the concordant curve in the  $^{207}\text{Pb}/^{235}\text{U}$  versus  $^{206}\text{Pb}/^{238}\text{U}$  concordia diagram ([Fig. 4](#)). The youngest and oldest ages were 36 Ma (CK01-D4-3) and 2 138.9 Ma (CK01-D5-2), respectively. Mesozoic ages were common in this sample (146.1–105.7 Ma, eight grains). The

Neoproterozoic ages range from 884.1 Ma to 623.4 Ma (nine grains). In addition, there was one Paleozoic zircon grain (300.2 Ma, CK01-D4-2).

## 5 Discussions

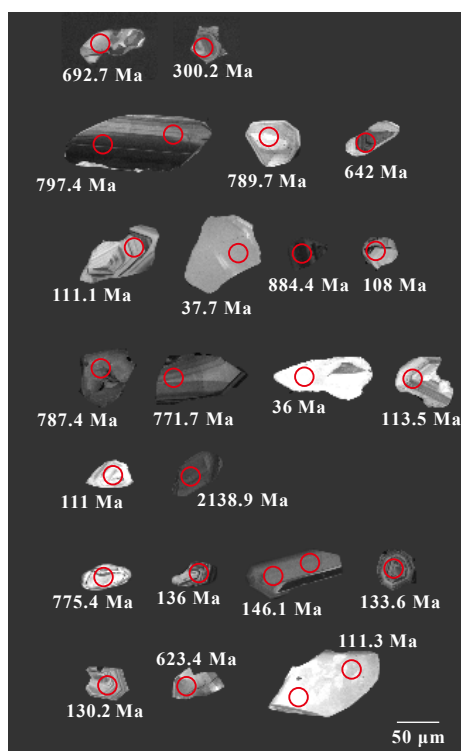
### 5.1 Basaltic pyroclastic rocks property

Pyroclastic rocks are formed when the pyroclastic material from volcanic eruptions is transported, deposited, and consolidated with air or water ([Sun et al., 2001; Zhou et al., 2022](#)). It is a transitional-type rock between lava and sedimentary rocks ([Sun et al., 2001](#)). The basement of Well CK-1 was composed of basaltic pyroclastic rocks. We suggest that the basaltic pyroclastic rocks from Well CK-1 are pyroclastic rocks on the seamount, based on the following lines of evidence:

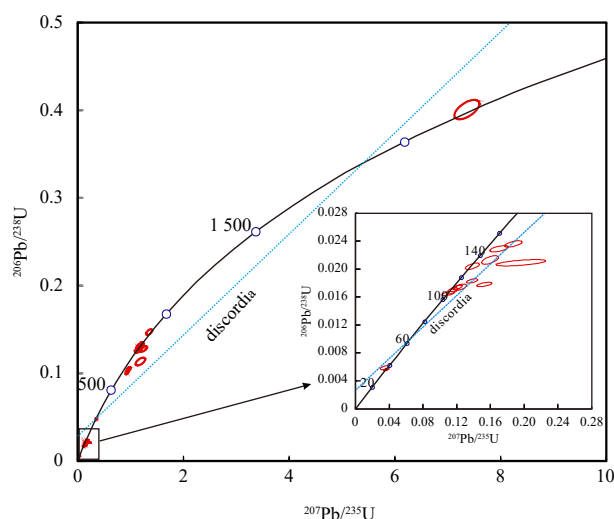
(1) The petrographic research results show that the composition of basaltic pyroclastic rocks is single, and there is an absence of terrigenous detritus within the pyroclastic rocks (e.g., quartz), which is consistent with the characteristics of pyroclastic rocks on seamounts ([Yan and Shi, 2009; Fan et al., 2021a, 2021b](#)). The pyroclastic rock on the seamount was a product of subaqueous explosive volcanism ([Fouquet et al., 1998; Davis and Clague, 2006; Yan and Shi, 2009](#)). If the depth of the magmatic eruption is greater than the pressure compensation depth, explosive volcanism can occur, producing volcanoclastic sediments. The positive topography at the top of the seamount limited the arrival of exo-

**Table 1.** LA-ICP-MS zircon U-Pb isotope data the basaltic pyroclastic rocks from Well CK-1

| Sports      | Th/<br>10 <sup>-6</sup> | U/<br>10 <sup>-6</sup> | Th/U | Isotopic ratios(1σ)                     |         |  |         |  |         | Apparent ages/Ma                        |       |  |      |  |      | Concordance |
|-------------|-------------------------|------------------------|------|---|---------|--|---------|--|---------|---|-------|--|------|--|------|-------------|
|             |                         |                        |      | <sup>207</sup> Pb/<br><sup>206</sup> Pb | 1σ      | <sup>207</sup> Pb/<br><sup>235</sup> U | 1σ      | <sup>206</sup> Pb/<br><sup>238</sup> U | 1σ      | <sup>207</sup> Pb/<br><sup>206</sup> Pb | 1σ    | <sup>207</sup> Pb/<br><sup>235</sup> U | 1σ   | <sup>206</sup> Pb/<br><sup>238</sup> U | 1σ   |             |
| CKO1-D1-1   | 401                     | 247                    | 1.62 | 0.075 3                                 | 0.001 8 | 1.187 0                                | 0.037 0 | 0.113 4                                | 0.001 8 | 1 075.9                                 | 47.4  | 794.6                                  | 17.2 | 692.7                                  | 10.6 | 86%         |
| CKO1-D1-2   | 303                     | 292                    | 1.04 | 0.053 0                                 | 0.001 1 | 0.348 6                                | 0.007 6 | 0.047 7                                | 0.000 5 | 331.5                                   | 46.3  | 303.6                                  | 5.8  | 300.2                                  | 3.2  | 98%         |
| CKO1-D2-1   | 283                     | 312                    | 0.91 | 0.065 5                                 | 0.000 7 | 1.197 3                                | 0.017 8 | 0.132 2                                | 0.001 4 | 790.7                                   | 24.1  | 799.4                                  | 8.2  | 800.2                                  | 8.1  | 99%         |
| CKO1-D2-1-2 | 335                     | 369                    | 0.91 | 0.065 8                                 | 0.000 8 | 1.193 7                                | 0.020 4 | 0.131 2                                | 0.001 6 | 799.7                                   | 25.9  | 797.7                                  | 9.5  | 794.6                                  | 9.3  | 99%         |
| CKO1-D2-2   | 203                     | 257                    | 0.79 | 0.063 7                                 | 0.000 8 | 1.148 2                                | 0.017 8 | 0.130 4                                | 0.001 3 | 731.5                                   | 27.8  | 776.4                                  | 8.4  | 789.9                                  | 7.5  | 98%         |
| CKO1-D2-3   | 514                     | 371                    | 1.39 | 0.066 6                                 | 0.000 9 | 0.965 0                                | 0.016 1 | 0.104 7                                | 0.001 0 | 833.3                                   | 29.6  | 685.9                                  | 8.3  | 642.0                                  | 6.1  | 93%         |
| CKO1-D3-1   | 191                     | 302                    | 0.63 | 0.050 4                                 | 0.001 5 | 0.120 8                                | 0.003 7 | 0.017 4                                | 0.000 2 | 216.7                                   | 70.4  | 115.8                                  | 3.3  | 111.1                                  | 1.3  | 95%         |
| CKO1-D3-2   | 57                      | 51                     | 1.13 | 0.058 6                                 | 0.008 7 | 0.035 1                                | 0.003 9 | 0.005 9                                | 0.000 2 | 553.7                                   | 330.5 | 35.0                                   | 3.8  | 37.7                                   | 1.4  | 92%         |
| CKO1-D3-3   | 65                      | 155                    | 0.42 | 0.066 6                                 | 0.001 1 | 1.352 9                                | 0.023 5 | 0.147 0                                | 0.001 4 | 833.3                                   | 33.3  | 868.8                                  | 10.1 | 884.1                                  | 7.7  | 98%         |
| CKO1-D3-4   | 181                     | 349                    | 0.52 | 0.049 9                                 | 0.001 9 | 0.114 8                                | 0.004 3 | 0.016 9                                | 0.000 3 | 190.8                                   | 87.0  | 110.4                                  | 3.9  | 108.0                                  | 2.1  | 97%         |
| CKO1-D4-1   | 84                      | 113                    | 0.74 | 0.066 4                                 | 0.001 2 | 1.188 6                                | 0.022 0 | 0.129 9                                | 0.001 3 | 818.2                                   | 32.4  | 795.3                                  | 10.2 | 787.4                                  | 7.7  | 98%         |
| CKO1-D4-2   | 35                      | 49                     | 0.72 | 0.065 8                                 | 0.001 6 | 1.151 4                                | 0.029 2 | 0.127 2                                | 0.001 6 | 1 200.0                                 | 51.9  | 777.9                                  | 13.8 | 771.7                                  | 8.9  | 99%         |
| CKO1-D4-3   | 459                     | 539                    | 0.85 | 0.047 1                                 | 0.002 8 | 0.036 1                                | 0.002 0 | 0.005 6                                | 0.000 1 | 57.5                                    | 133.3 | 36.0                                   | 2.0  | 36.0                                   | 0.6  | 99%         |
| CKO1-D4-4   | 132                     | 236                    | 0.56 | 0.062 6                                 | 0.002 4 | 0.152 8                                | 0.006 0 | 0.017 8                                | 0.000 2 | 696.0                                   | 82.6  | 144.4                                  | 5.3  | 113.5                                  | 1.5  | 76%         |
| CKO1-D5-1   | 250                     | 265                    | 0.94 | 0.051 6                                 | 0.001 9 | 0.124 0                                | 0.005 0 | 0.017 4                                | 0.000 3 | 333.4                                   | 83.3  | 118.7                                  | 4.5  | 111.0                                  | 1.7  | 93%         |
| CKO1-D5-2   | 204                     | 284                    | 0.72 | 0.133 0                                 | 0.001 1 | 7.362 9                                | 0.096 4 | 0.400 7                                | 0.004 5 | 2 138.9                                 | 13.9  | 2 156.5                                | 11.8 | 2 172.1                                | 20.8 | 99%         |
| CKO1-D6-1   | 133                     | 112                    | 1.19 | 0.070 5                                 | 0.001 6 | 1.242 9                                | 0.028 5 | 0.127 8                                | 0.001 3 | 942.6                                   | 46.3  | 820.2                                  | 12.9 | 775.4                                  | 7.6  | 94%         |
| CKO1-D6-2   | 142                     | 153                    | 0.93 | 0.056 2                                 | 0.002 6 | 0.159 5                                | 0.006 6 | 0.021 3                                | 0.000 4 | 457.5                                   | 106.5 | 150.2                                  | 5.8  | 136.0                                  | 2.3  | 90%         |
| CKO1-D6-3   | 255                     | 215                    | 1.19 | 0.053 9                                 | 0.002 2 | 0.170 2                                | 0.007 3 | 0.022 9                                | 0.000 3 | 368.6                                   | 92.6  | 159.6                                  | 6.3  | 146.1                                  | 1.7  | 91%         |
| CKO1-D6-3-2 | 274                     | 228                    | 1.20 | 0.057 8                                 | 0.002 1 | 0.187 2                                | 0.006 9 | 0.023 6                                | 0.000 3 | 524.1                                   | 77.8  | 174.2                                  | 5.9  | 150.3                                  | 1.8  | 85%         |
| CKO1-D6-5   | 237                     | 281                    | 0.85 | 0.067 8                                 | 0.006 4 | 0.196 1                                | 0.019 5 | 0.020 9                                | 0.000 3 | 864.8                                   | 199.1 | 181.8                                  | 16.5 | 133.6                                  | 1.7  | 69%         |
| CKO1-D7-1   | 153                     | 222                    | 0.69 | 0.049 0                                 | 0.001 8 | 0.138 5                                | 0.005 5 | 0.020 4                                | 0.000 3 | 146.4                                   | 87.0  | 131.7                                  | 4.9  | 130.2                                  | 1.8  | 98%         |
| CKO1-D7-2   | 760                     | 568                    | 1.34 | 0.066 8                                 | 0.000 9 | 0.937 1                                | 0.014 5 | 0.101 5                                | 0.001 1 | 831.5                                   | 25.9  | 671.4                                  | 7.6  | 623.4                                  | 6.7  | 92%         |
| CKO1-D7-3   | 147                     | 263                    | 0.56 | 0.054 8                                 | 0.001 8 | 0.138 2                                | 0.004 5 | 0.018 3                                | 0.000 2 | 405.6                                   | 74.1  | 131.4                                  | 4.1  | 116.9                                  | 1.4  | 88%         |
| CKO1-D7-3-3 | 119                     | 222                    | 0.53 | 0.048 2                                 | 0.002 2 | 0.109 9                                | 0.005 0 | 0.016 5                                | 0.000 2 | 109.4                                   | 107.4 | 105.9                                  | 4.5  | 105.7                                  | 1.4  | 99%         |

**Fig. 3.** CL images for U-Pb dated zircons for the basaltic pyroclastic rocks from Well CK-1.

genous debris, making the composition of pyroclastic rocks on the seamount relatively singular, except for a small number of biological remains carried in a suspended manner (Yan and Shi,

**Fig. 4.** Zircon U-Pb Concordia plots for the basaltic pyroclastic rocks from Well CK-1.

2009). The size and quantity of biological remains are small compared to those of pyroclasts in pyroclastic rocks on seamounts (Zhang et al., 2014). Furthermore, the crystal clastic minerals are subangular or angular, mixed in size, and broken into steps or jagged shapes along the cleavage plane (Fig.2), suggesting that the basaltic pyroclastic rocks from Well CK-1 may have been deposited *in situ*.

(2) The thickness of the basaltic pyroclastic rocks from Chenhang Island is more than 52 m (Zhang et al., 2018, 2020b). If they were transported over long distances by air or water, they would

have been widely distributed on the Xisha Islands. However, Wells XY-1 and XK-1, which are adjacent to Well CK-2 (Fig. 1), penetrated the thick coral reef limestone into the underlying metamorphic basement. Similar basaltic volcanic clastic rocks are not found in either well (Wells XY-1 and XK-1), indicating that the basaltic pyroclastic rocks were deposited *in situ*.

(3) Huang et al. (2011a, 2011b) installed temporary earthquake stations on Chenhang Island. Based on earthquake observations and the onshore-offshore seismic experiments, Huang et al. (2011a) suggested that the thickness of the Earth's crust reaches its maximum beneath Chenhang Island and gradually decreases outward. Huang et al. (2011b) used natural seismic data from Chenhang Island to simulate the crustal structure and found that the lower crust has a ductile rheological structure caused by the deep thermal activity of the mantle.

(4) The depocenter around the Xisha Uplift (Huaguang Depression, Qiongdongnan Basin, Zhongjiannan Basin, and Xisha Trough) prevents exotic pyroclastic material from being deposited in the adjacent areas of the Xisha Uplift (Fig. 1), which further indicates that the pyroclastic material could not be transported over long distances by water.

In summary, we suggest that the basaltic pyroclastic rocks from Well CK-1 are pyroclastic rocks of the seamount. Based on the geophysical data in the Xisha area and its adjacent areas, Zhang et al., identified flat-topped and conical-topped seamounts in the Xisha area. The flat-topped seamount is characterized by a flat and wide top, but a steep slope. Magnetic anomalies suggest that the flat-topped seamount may be basaltic in nature rather than continental crust or shallow-water sandstone deposits. The conical-topped seamounts are thought to have been formed by a strong central eruption of the volcano. In contrast to flat-topped seamounts, conical-topped seamounts have high and sharp heads exposed above the seafloor (Zhang et al., 2014, 2016). We further speculated that Chenhang Island may be one of the seamounts described by Zhang et al. (2014, 2016). After the Miocene, the Xisha Islands began to sink and were gradually submerged. Consequently, the area has suitable temperature, salinity and water depth, and coral reef strata have been extensively developed.

### 5.2 The age of the basaltic volcanic clastic rocks

Precise dating of basic volcanic rocks, particularly young basic volcanic rocks, is an important scientific problem that has long plagued geologists. Si and Zr are normally unsaturated in basic rocks. Zircons in basic volcanic rocks usually have multiple geneses, particularly in young samples. They may have crystallized in the magma reservoirs from which the rocks were derived or may have been trapped from the wall rock through which the magma was raised (Hanchar and Hoskin, 2003; Song and Qiao, 2008; Pereira et al., 2011). Volcanic eruption events are instantaneous during geological evolution, and it is difficult to simultaneously form contemporaneous zircons with basaltic eruptions. Most zircon grains in basic volcanic rocks, especially larger zircon grains, are formed in the magma chamber or captured during the upward migration of magma through a conduit (Song and Qiao, 2008). If sufficient zircon grains are analyzed in volcanic rocks, the youngest ages among them would be nearest to the age of the volcanic eruption and could be regarded as a maximum estimation of the age of the volcanic eruption (Song and Qiao, 2008).

In this study, the youngest zircon ages were considered as the maximum ages of the basalt eruption. Two Cenozoic zircons from Well CK-1 gave a weighted mean  $^{206}\text{Pb}/^{238}\text{U}$  age of  $36.3 \pm 1.1$  Ma Mean Squared Weighted Deviation [(MSWD) = 1.2],

which may represent the maximum age of the volcano eruption. Furthermore, there are eight Cenozoic zircon grains from Well CK-2, which gave a weighted mean  $^{206}\text{Pb}/^{238}\text{U}$  age of  $(35.5 \pm 0.9)$  Ma (Zhang et al., 2020b), which is consistent with our study within error. Therefore, we suggest that the age of the basaltic volcanic eruption beneath Chenhang Island was as early as 36 Ma.

### 5.3 Basement nature of Xisha micro-block

As discussed in Section 5.1, the basaltic pyroclastic rocks from Well CK-1 were pyroclastic rocks on the seamount. The older zircon grains from Well CK-1 were inherited zircons rather than being detrital zircons. Information obtained from inherited zircons is crucial for decrypting the time intervals of older magmatic events that are poorly exposed on the crustal surface. The inherited zircons can be used to indicate concealed magmatic events (Zheng et al., 2006; Condie et al., 2009; Pereira et al., 2011; Pan et al., 2014; Zhu et al., 2016; Wang et al., 2020).

The inherited zircons from Well CK-1 displayed three major age groups: 116.9–105.7 Ma, 146.1–130.2 Ma, and 884.1–623.4 Ma. Late Mesozoic Yanshanian igneous activity was widely dispersed in the SCS and its surrounding areas, such as the Nansha, Zhongsha, and Xisha micro-blocks, and Pearl River Mouth Basin (Jin, 1989; Li et al., 1999; Qiu et al., 2008; Yan et al., 2008a, 2010, 2014, Shi et al., 2011; Wang et al., 2015; Zhu et al., 2017 and references therein). It is generally accepted that these Late Mesozoic magmatic activities are related to the subduction of the Paleo-Pacific Plate beneath the Eurasian Plate (Zhou and Li, 2000; Li et al., 2007a, 2018; Li and Li, 2007; Chen et al., 2008; Shi et al., 2011; Yan et al., 2014; Xu et al., 2017; Yuan et al., 2018 and references therein).

The ages of the late Mesozoic Yanshanian igneous rocks from the SCS region range from 159 Ma to 70.5 Ma, indicating that the late Mesozoic igneous activity in the SCS lasted for a long time (Yan et al., 2014). The magmatic ages of the granitic rocks from the Nansha micro-block varied from 159 to 127 Ma, implying the existence of a continental basement within the Nansha micro-block (Yan et al., 2010). Fine-grained biotite granite was dredged from the southwestern SCS Basin. K-Ar, Ar-Ar, and U-Pb dating showed that these granites formed during the Early Cretaceous (120–109.7 Ma) (Qiu et al., 2008). In the northern SCS basin, many boreholes have been drilled into the basement metamorphic rocks (e.g., P1-1-1 and YJ35-1-1 from the Pearl River Mouth Basin; HK17-1-1 and HK30-3-1A from the Yinggehai Basin; WZ23-3-1, WS31-1-1, and WS26-4-1 from the Beibu Gulf Basin; and BD15-3-1 and YC13-4-1 from the Qiongdongnan Basin). However, owing to the lack of high-precision dating and stratigraphic sequences, it is not yet possible to distinguish whether they are Precambrian crystalline basements or late-stage tectonic metamorphisms (Sun et al., 2014). Jin (1989) identified biotite-plagioclase gneiss in the basement of the Zhongsha micro-block. The biotite and plagioclase from the metamorphic rocks yielded K-Ar ages of 127–119 Ma (Jin, 1989), which is consistent with Early Cretaceous igneous activity in southeastern China (Zhou and Li, 2000; Shi et al., 2011). Kudrass et al. (1986) reported the Jurassic–Cretaceous metamorphic rocks dredged from Reed Bank. The K-Ar ages of these samples were 146 Ma, 122 Ma, and 113 Ma for the amphibolite, paragneiss, and phyllite, respectively (Kudrass et al., 1986).

Well XK-1 is located 80 km from CK-1. Its basement comprised of Late Jurassic amphibole plagioclase gneiss ( $152.9 \pm 1.7$  Ma) and was intruded by late Early Cretaceous granitic magma [(107.8  $\pm$  3.6) Ma] (Zhu et al., 2017). Based on the presence of contemporaneous metamorphic rocks in the SCS, Zhu et

al. (2017) suggested the presence of an E–W trending metamorphic zone within the northern SCS during the Cretaceous. The Late Mesozoic inherited zircons (116.9–105.7 Ma and 146.1–130.2 Ma) from Well CK-1 are consistent with the zircons from Well XK-1. There were two peak periods of Yanshanian igneous activity in southeastern China (195–150 Ma and 131–117 Ma) (Wu et al., 2005a, 2005b). Similar zircon ages indicate that late Mesozoic magmatism in the Xisha micro-block is consistent with that in southeastern China and imply that the northern SCS area may have a geodynamic setting similar to that of southeastern China during the Mesozoic. Combined with the zircon U–Pb ages from CK-2 (Fig. 5), we further speculate that the basement of Chenhang Island may be similar to that of Well XK-1. As the Cenozoic basaltic volcanic eruption on Chenhang Is-

land, the Late Mesozoic zircons were preserved in the basaltic pyroclastic rocks in the form of inherited zircons. The Xisha micro-block may have developed on a uniform Late Jurassic metamorphic crystalline basement intruded by the Cretaceous granitic magma (Fig. 6).

Furthermore, several Neoproterozoic zircons were present in this study (884.1–623.4 Ma). A similar Neoproterozoic inherited zircon (675 Ma) was identified from the granitic rocks in the Nansha micro-block, which may have been produced by the partial melting of the older Precambrian basement (Yan et al., 2008b, 2010). The crustal remelting of the old Precambrian basement corresponds to the rapid thinning of the South China lithosphere during the Mesozoic, which covered the imprint of the Precambrian crystalline basement in the study area (Wan, 2004; Xu, 2008).

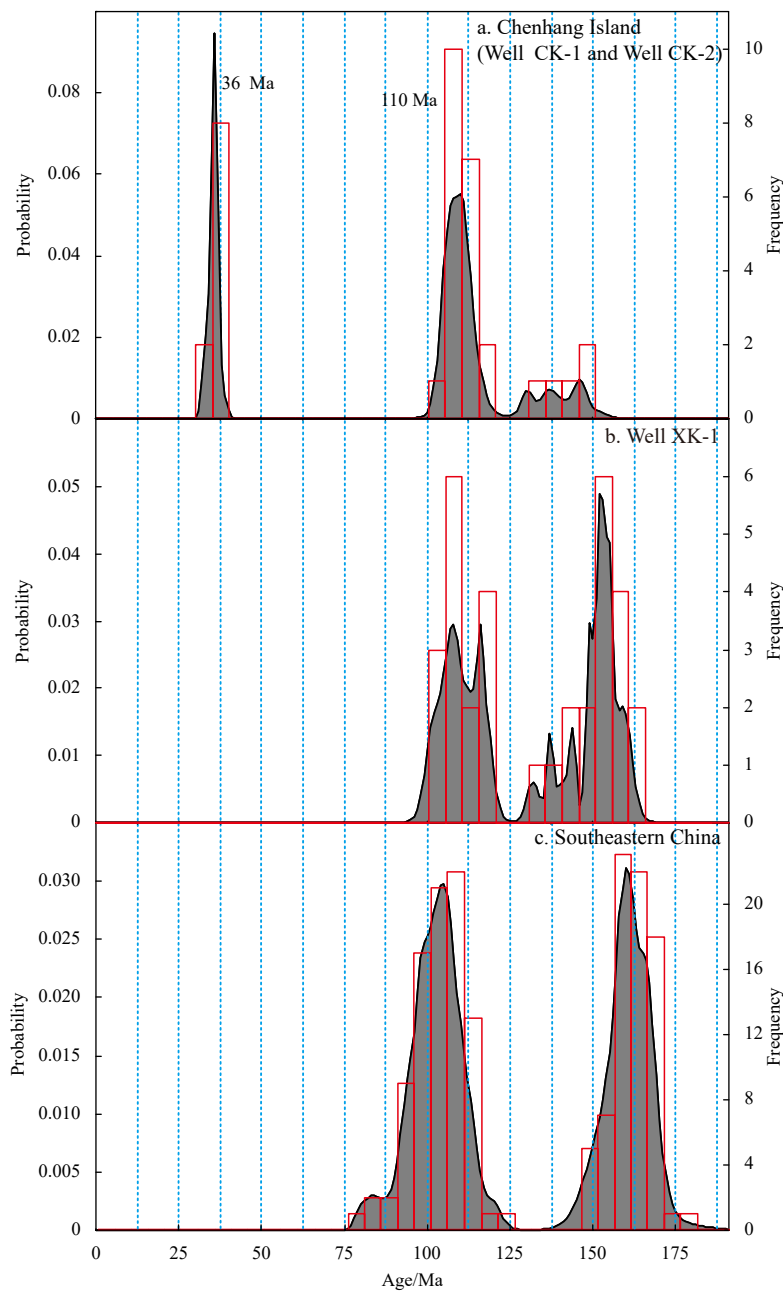


**Fig. 5.** Relative probability density diagram of ages for the analyzed samples along with compiled plots from surrounding areas. a. Chenhang Island (Well CK-1 and Well CK-2). Data sources are Zhang et al. (2020b); b. Well XK-1. Data sources are Zhu et al. (2017). c. Southeastern China. Data sources are Li et al. (2007b) and Yuan et al. (2019).

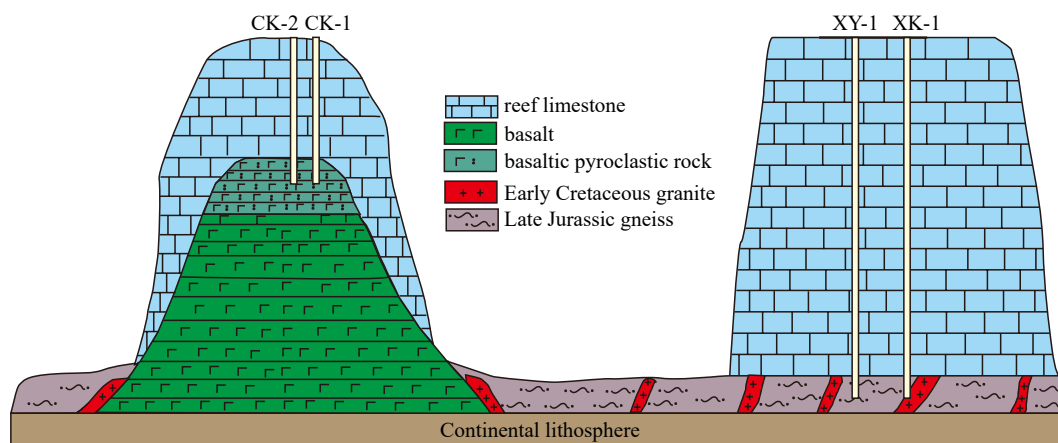


Fig. 6. Schematic diagram for the basement of Xisha Islands.

## 6 Conclusions

The basement of Well CK-1 consists of basaltic pyroclastic rocks on the seamount. LA-ICP-MS U-Pb dating showed that the basaltic volcanic eruption occurred as early as 36 Ma. The Xisha micro-block may have developed on a uniform Late Jurassic metamorphic crystalline basement intruded by the Cretaceous granitic magma.

## Acknowledgements

We are grateful to two anonymous reviewers who provided constructive suggestions regarding an earlier version of the paper.

## References

- Briaux A, Patriat P, Tapponnier P. 1993. Updated interpretation of magnetic anomalies and seafloor spreading stages in the South China Sea: implications for the tertiary tectonics of Southeast Asia. *Journal of Geophysical Research: Solid Earth*, 98(B4): 6299–6328, doi: [10.1029/92JB02280](https://doi.org/10.1029/92JB02280)
- Chen Chenghong, Lee C Y, Shinjo R. 2008. Was there Jurassic paleo-Pacific subduction in South China?: constraints from  $^{40}\text{Ar}/^{39}\text{Ar}$  dating, elemental and Sr-Nd-Pb isotopic geochemistry of the Mesozoic basalts. *Lithos*, 106(1–2): 83–92, doi: [10.1016/j.lithos.2008.06.009](https://doi.org/10.1016/j.lithos.2008.06.009)
- Chen Haiyun, Yu Jianguo, Shu Liangshu, et al. 2005. The structural styles and their relation with petroleum-gas resources of the Jiyang depression, Shandong province, China. *Geological Journal of China Universities (in Chinese)*, 11(4): 622–632
- Compiled by the Second Marine Geological Investigation Brigade of the Ministry of Geology and Mineral Resources. 1987. *Atlas of Geology and Geophysics of South China Sea (in Chinese)*. Guangzhou: Map Publishing House of Guangdong Province
- Condie K C, Belousova E, Griffin W L, et al. 2009. Granitoid events in space and time: constraints from igneous and detrital zircon age spectra. *Gondwana Research*, 15(3–4): 228–242, doi: [10.1016/j.gr.2008.06.001](https://doi.org/10.1016/j.gr.2008.06.001)
- Davis A S, Clague D A. 2006. Volcaniclastic deposits from the North Arch volcanic field, Hawaii: explosive fragmentation of Alkalic lava at abyssal depths. *Bulletin of Volcanology*, 68(3): 294–307, doi: [10.1007/s00445-005-0008-7](https://doi.org/10.1007/s00445-005-0008-7)
- Deng Jun, Wang Qingfei, Huang Dinghua, et al. 2005. Basement evolution of the Ordos Basin and its constraint on cap rock. *Earth Science Frontiers (in Chinese)*, 12(3): 91–99
- Fan Jianjun, Li Cai, Niu Yaoling, et al. 2021b. Identification method and geological significance of intraplate ocean island-seamount fragments in orogenic belt. *Earth Science (in Chinese)*, 46(2): 381–404
- Fan Jianjun, Niu Yaoling, Liu Yiming, et al. 2021a. Timing of closure of the Meso-Tethys Ocean: constraints from remnants of a 141–135 Ma ocean island within the Bangong-Nujiang Suture Zone, Tibetan Plateau. *GSA Bulletin*, 133(9–10): 1875–1889, doi: [10.1130/B35896.1](https://doi.org/10.1130/B35896.1)
- Fang Penggao, Ding Weiwei, Fang Yinxia, et al. 2017. Cenozoic tectonic subsidence in the southern continental margin, South China Sea. *Frontiers of Earth Science*, 11(2): 427–441, doi: [10.1007/s11707-016-0594-z](https://doi.org/10.1007/s11707-016-0594-z)
- Fouquet Y, Eissen J P, Ondréas H, et al. 1998. Extensive volcanoclastic deposits at the Mid-Atlantic Ridge axis: results of deep-water basaltic explosive volcanic activity? *Terra Nova*, 10(2): 280–286, doi: [10.1046/J.1365-3121.1998.00204.X](https://doi.org/10.1046/J.1365-3121.1998.00204.X)
- Gao Fuhong, Xu Wenliang, Yang Debin, et al. 2007. LA-ICP-MS zircon U-Pb dating from granitoids in southern basement of Songliao basin: constraints on ages of the basin basement. *Science in China Series D: Earth Sciences*, 50(7): 995–1004, doi: [10.1007/s11430-007-0019-7](https://doi.org/10.1007/s11430-007-0019-7)
- Guo Lingli, Li Sanzhong, Zhao Shujuan, et al. 2016a. Final breakup of continental block and opening of oceanic lithosphere: insights from deep crustal structure and tectonic evolution of the ocean-continent transition zone in the northern South China Sea. *Geological Journal*, 51(S1): 318–330, doi: [10.1002/gj.2842](https://doi.org/10.1002/gj.2842)
- Guo Xiaoran, Zhao Minghui, Huang Haibo, et al. 2016b. Crustal structure of Xisha block and its tectonic attributes. *Chinese Journal of Geophysics (in Chinese)*, 59(4): 1414–1425
- Guynn J, Kapp P, Gehrels G E, et al. 2012. U-Pb geochronology of basement rocks in central Tibet and paleogeographic implications. *Journal of Asian Earth Sciences*, 43(1): 23–50, doi: [10.1016/j.jseaes.2011.09.003](https://doi.org/10.1016/j.jseaes.2011.09.003)
- Hanchar J M, Hoskin P W O. 2003. Zircon. *Reviews in Mineralogy and Geochemistry*, 53: 500
- Hao Tianyao, Xu Ya, Zhao Baimin, et al. 2009. Geophysical research on distribution features of magnetic basements in the South China Sea. *Chinese Journal of Geophysics (in Chinese)*, 52(11): 2763–2774
- He Dengfa, Ma Yongsheng, Cai Xunyu, et al. 2017. Comparison study on controls of geologic structural framework upon hydrocarbon distribution of marine basins in western China. *Acta Petrologica Sinica (in Chinese)*, 33(4): 1037–1057
- Huang Haibo, Qiu Xuelin, Xu Huilong, et al. 2011a. Preliminary results of the earthquake observation and the onshore-offshore seismic experiments on Xisha Block. *Chinese Journal of Geophysics (in Chinese)*, 54(12): 3161–3170, doi: [10.3969/j.issn.0001-5733.2011.12.016](https://doi.org/10.3969/j.issn.0001-5733.2011.12.016)
- Huang Haibo, Qiu Xuening, Xu Yi, et al. 2011b. Crustal structure beneath the Xisha Islands of the South China Sea simulated by the teleseismic receiver function method. *Chinese Journal of Geophysics (in Chinese)*, 54(11): 2788–2798, doi: [10.3969/j.issn.0001-5733.2011.11.009](https://doi.org/10.3969/j.issn.0001-5733.2011.11.009)
- Jin Xianglong. 1989. *Geosciences study of South China Sea*. Donghai Marine Science (in Chinese), 7(4): 1–92
- Kudrass H R, Wiedicke M, Cepek P, et al. 1986. Mesozoic and Caino-

- zoic rocks dredged from the South China Sea (Reed Bank area) and Sulu Sea and their significance for plate-tectonic reconstructions. *Marine and Petroleum Geology*, 3(1): 19–30, doi: [10.1016/0264-8172\(86\)90053-X](https://doi.org/10.1016/0264-8172(86)90053-X)
- Li Jianhua, Dong Shuwen, Cawood P A, et al. 2018. An Andean-type retro-arc foreland system beneath northwest South China revealed by SINOPROBE profiling. *Earth and Planetary Science Letters*, 490: 170–179, doi: [10.1016/j.epsl.2018.03.008](https://doi.org/10.1016/j.epsl.2018.03.008)
- Li Zhengxiang, Li Xianhua. 2007. Formation of the 1300-km-wide intracontinental orogen and postorogenic magmatic province in Mesozoic South China: a flat-slab subduction model. *Geology*, 35(2): 179–182, doi: [10.1130/G23193A.1](https://doi.org/10.1130/G23193A.1)
- Li Chunfeng, Li Jiabiao, Ding Weiwei, et al. 2015. Seismic stratigraphy of the central South China Sea basin and implications for neotectonics. *Journal of Geophysical Research: Solid Earth*, 120(3): 1377–1399, doi: [10.1002/2014JB011686](https://doi.org/10.1002/2014JB011686)
- Li Xianhua, Li Wuxian, Li Zhengxiang. 2007a. On the genetic classification and tectonic implications of the Early Yanshanian granitoids in the Nanling Range, South China. *Chinese Science Bulletin*, 52(14): 1873–1885, doi: [10.1007/s11434-007-0259-0](https://doi.org/10.1007/s11434-007-0259-0)
- Li Xianhua, Li Zhengxiang, Li Wuxian, et al. 2007b. U-Pb zircon, geochemical and Sr–Nd–Hf isotopic constraints on age and origin of Jurassic I- and A-type granites from central Guangdong, SE China: a major igneous event in response to foundering of a subducted flat-slab? *Lithos*, 96(1–2): 186–204, doi: [10.1016/j.lithos.2006.09.018](https://doi.org/10.1016/j.lithos.2006.09.018)
- Li Pinglu, Liang Huixian, Dai Yiding, et al. 1999. Origin and tectonic setting of the Yanshanian igneous rocks in the Pearl River Mouth basin. *Guangdong Geology (in Chinese)*, 14(1): 1–8
- Li Chunfeng, Xu Xing, Lin Jian, et al. 2014. Ages and magnetic structures of the South China Sea constrained by deep tow magnetic surveys and IODP Expedition 349. *Geochemistry, Geophysics, Geosystems*, 15(12): 4958–4983, doi: [10.1002/2014GCO005567](https://doi.org/10.1002/2014GCO005567)
- Li Naisheng, Yan Quanshu, Chen Zhihua, et al. 2013. Geochemistry and petrogenesis of Quaternary volcanism from the islets in the eastern Beibu Gulf: evidence for Hainan plume. *Acta Oceanologica Sinica*, 32(12): 40–49, doi: [10.1007/s13131-013-0386-1](https://doi.org/10.1007/s13131-013-0386-1)
- Li Ming, Yan Lei, Han Shaoyang. 2012. The basement tectonic characteristics in Ordos Basin. *Journal of Jilin University (Earth Science Edition) (in Chinese)*, 42(S3): 38–43
- Li Shiyang, Yu Kefu, Zhang Yu, et al. 2019. Mineral chemistry of clinopyroxene in pyroclastic rocks of the Xisha Islands and their geological significance. *Haiyang Xuebao (in Chinese)*, 41(7): 65–76, doi: [10.3969/j.issn.0253-4193.2019.07.006](https://doi.org/10.3969/j.issn.0253-4193.2019.07.006)
- Lin Changsong, Chu Fengyou, Gao Jinyao, et al. 2009. On tectonic movement in the South China Sea during the Cenozoic. *Acta Oceanologica Sinica*, 28(1): 25–36
- Liu Yongsheng, Gao Shan, Hu Zhaochu, et al. 2010. Continental and oceanic crust recycling-induced melt-peridotite interactions in the Trans-North China Orogen: U-Pb dating, Hf isotopes and trace elements in zircons from mantle xenoliths. *Journal of Petrology*, 51(1–2): 537–571, doi: [10.1093/petrology/egp082](https://doi.org/10.1093/petrology/egp082)
- Liu Yongsheng, Hu Zhaochu, Gao Shan, et al. 2008. *In situ* analysis of major and trace elements of anhydrous minerals by LA-ICP-MS without applying an internal standard. *Chemical Geology*, 257(1–2): 34–43, doi: [10.1016/j.chemgeo.2008.08.004](https://doi.org/10.1016/j.chemgeo.2008.08.004)
- Liu Hailing, Sun Yan, Guo Lingzhi, et al. 1999. On the kinematic characteristics and dynamic process of boundary faults of the Nansha ultra-crust layer-block. *Acta Geologica Sinica (English Edition)*, 73(4): 452–463, doi: [10.1111/j.1755-6724.1999.tb00855.x](https://doi.org/10.1111/j.1755-6724.1999.tb00855.x)
- Liu Hailing, Yan Pin, Liu Yingchun, et al. 2006. Existence of Qiongnan suture zone on the north margin of South China Sea. *Chinese Science Bulletin*, 51(S2): 107–120, doi: [10.1007/s11434-006-9107-x](https://doi.org/10.1007/s11434-006-9107-x)
- Liu Hailing, Yan Pin, Sun Yan, et al. 2002. Layer-block tectonics of the Nansha microplate. *Geology in China (in Chinese)*, 29(4): 374–381
- Liu Hailing, Yan Pin, Zhang Boyou, et al. 2004a. Pre-Cenozoic basements of the south china sea and eastern Tethyan realm. *Marine Geology & Quaternary Geology (in Chinese)*, 24(1): 15–28
- Liu Hailing, Yang Tian, Zhu Shufen, et al. 2004b. Tectonic evolution of Cenozoic sedimentary basements in the northwestern South China Sea. *Haiyang Xuebao (in Chinese)*, 26(3): 54–67
- Liu Yixuan, Zhan Wenhui. 1994. Basic outline and tectonic evolution of the metamorphic basement in the South China Sea. *Geology of Anhui (in Chinese)*, 4(1–2): 82–90
- Liu Hailing, Zheng Hongbo, Wang Yanlin, et al. 2011. Basement of the South China Sea area: tracing the Tethyan Realm. *Acta Geologica Sinica (English Edition)*, 85(3): 637–655, doi: [10.1111/j.1755-6724.2011.00457.x](https://doi.org/10.1111/j.1755-6724.2011.00457.x)
- Lu Baoliang, Wang Pujun, Zhang Gongcheng, et al. 2011. Basement structures of an epicontinental basin in the northern South China Sea and their significance in petroleum prospect. *Acta Petrologica Sinica (in Chinese)*, 32(4): 580–587
- Ludwig K R. 2003. *User's Manual for Isoplot 3.00: A Geochronological Toolkit for Microsoft Excel*. Berkeley: Berkeley Geochronology Center
- Miao Xiuquan, Huang Xiaolong, Yan Wen, et al. 2021. Late Triassic dacites from Well NK-1 in the Nansha Block: constraints on the Mesozoic tectonic evolution of the southern South China Sea margin. *Lithos*, 398–399: 106337, doi: [10.1016/j.lithos.2021.106337](https://doi.org/10.1016/j.lithos.2021.106337)
- Mora-Bohórquez J A, Ibáñez-Mejía M, Oncken O, et al. 2017. Structure and age of the Lower Magdalena Valley basin basement, northern Colombia: new reflection-seismic and U-Pb-Hf insights into the termination of the central Andes against the Caribbean basin. *Journal of South American Earth Sciences*, 74: 1–26, doi: [10.1016/j.jsames.2017.01.001](https://doi.org/10.1016/j.jsames.2017.01.001)
- Pan Shaokui, Zheng Jianping, Griffin W L, et al. 2014. Precambrian tectonic attribution and evolution of the Songliao terrane revealed by zircon xenocrysts from Cenozoic alkali basalts, Xilinhot region, NE China. *Precambrian Research*, 251: 33–48, doi: [10.1016/j.precamres.2014.05.022](https://doi.org/10.1016/j.precamres.2014.05.022)
- Pereira M F, Chichorro M, Solá A R, et al. 2011. Tracing the Cadomian magmatism with detrital/herited zircon ages by *in-situ* U-Pb SHRIMP geochronology (Ossa-Morena Zone, SW Iberian Massif). *Lithos*, 123(1–4): 204–217, doi: [10.1016/j.lithos.2010.11.008](https://doi.org/10.1016/j.lithos.2010.11.008)
- Qiu Yan, Chen Guoneng, Liu Fanglan, et al. 2008. Discovery of granite and its tectonic significance in southwestern basin of the South China Sea. *Geological Bulletin of China (in Chinese)*, 27(12): 2104–2107
- Qiu Xuelin, Zeng Gangping, Xu Yi, et al. 2006. The crustal structure beneath the Shidao station on Xisha Islands of South China Sea. *Chinese Journal of Geophysics (in Chinese)*, 49(6): 1720–1729, doi: [10.3321/j.issn:0001-5733.2006.06.019](https://doi.org/10.3321/j.issn:0001-5733.2006.06.019)
- Shi Hesheng, Xu Changlai, Zhou Zuyi, et al. 2011. Zircon U-Pb dating on granitoids from the Northern South China Sea and its geotectonic relevance. *Acta Geologica Sinica (English Edition)*, 85(6): 1359–1372, doi: [10.1111/j.1755-6724.2011.00592.x](https://doi.org/10.1111/j.1755-6724.2011.00592.x)
- Song Biao, Qiao Xiufu. 2008. Ages of zircons from basalt of erdaogou formation and diabase dyke swarms in Northern Liaoning. *Earth Science Frontiers*, 15(3): 250–262, doi: [10.1016/S1872-5791\(08\)60067-6](https://doi.org/10.1016/S1872-5791(08)60067-6)
- Sun Jiashi. 1987. A discussion on the formation ages of the bedrock in the Xisha islands. *Marine Geology & Quaternary Geology (in Chinese)*, (4): 5–6
- Sun Weidong. 2016. Initiation and evolution of the South China Sea: an overview. *Acta Geochimica*, 35(3): 215–225, doi: [10.1007/s11631-016-0110-x](https://doi.org/10.1007/s11631-016-0110-x)
- Sun Shanping, Liu Yongshun, Zhong Rong, et al. 2001. Classification of pyroclastic rocks and trend of volcanic sedimentology: a review. *Acta Petrologica et Mineralogica (in Chinese)*, 20(3): 313–317
- Sun Xiaomeng, Zhang Xuqing, Zhang Gongcheng, et al. 2014. Texture and tectonic attribute of Cenozoic basin basement in the northern South China Sea. *Science China Earth Sciences*, 57(6): 1199–1211, doi: [10.1007/s11430-014-4835-2](https://doi.org/10.1007/s11430-014-4835-2)
- Tang Li, Santosh M, Tsunogae T, et al. 2017. Petrology, phase equilibria modelling and zircon U-Pb geochronology of Paleoproterozoic mafic granulites from the Fuping Complex, North China Craton. *Journal of Metamorphic Geology*, 35(5): 517–540

- doi: [10.1111/jmg.12243](https://doi.org/10.1111/jmg.12243)
- Taylor B, Hayes D E. 1982. Origin and history of the South China Sea Basin. In: Hayes D E, ed. *The Tectonic and Geologic Evolution of Southeast Asian Seas and Islands: Part 2*. Washington: American Geophysical Union, 23–56
- Wan Tianfeng. 2004. Rotation of the Jurassic crust and transformation of the lithosphere in eastern China. *Geological Bulletin of China (in Chinese)*, 23(9–10): 966–972
- Wang Kai, Dong Shuwen, Yao Weihua, et al. 2020. Xenocrystic/inherited Precambrian zircons entrained within igneous rocks from eastern South China: tracking unexposed ancient crust and implications for late Paleoproterozoic orogenesis. *Gondwana Research*, 84: 194–210, doi: [10.1016/j.gr.2020.02.015](https://doi.org/10.1016/j.gr.2020.02.015)
- Wang Chongyou, He Xixian, Qiu Songyu. 1979. Carbonate stratigraphy and micropaleontology in Well Xi-Yong 1, Xisha Islands: a preliminary study. *Petroleum Geology & Experiment (in Chinese)*, 71: 2338 (in Chinese)
- Wang Wei, Ye Jiaren, Yang Xianghua, et al. 2015. Sediment provenance and depositional response to multi-stage rifting, Paleogene, Huizhou Depression, Pearl River Mouth Basin. *Earth Science-Journal of China University of Geosciences (in Chinese)*, 40(6): 10611071
- Wang Jian, Zhao Minghui, Qiu Xuelin, et al. 2016. 3D seismic structure of the Zhenbei-Huangyan seamounts chain in the East Sub-basin of the South China Sea and its mechanism of formation. *Geological Journal*, 51(S1): 448–463, doi: [10.1002/gj.2781](https://doi.org/10.1002/gj.2781)
- Wang Rui, Yu Kefu, Jones B, et al. 2018. Evolution and development of Miocene “island dolostones” on Xisha Islands, South China Sea. *Marine Geology*, 406: 142–158, doi: [10.1016/j.margeo.2018.09.006](https://doi.org/10.1016/j.margeo.2018.09.006)
- Wiedenbeck M, Allé P, Corfu F, et al. 1995. Three natural zircon standards for U-Th-Pb, Lu-Hf, trace element and REE analyses. *Geostandards and Geoanalytical Research*, 19(1): 1–23, doi: [10.1111/j.1751-908X.1995.tb00147.x](https://doi.org/10.1111/j.1751-908X.1995.tb00147.x)
- Wu Fuyuan, Lin Jingqian, Wilde S A, et al. 2005a. Nature and significance of the Early Cretaceous giant igneous event in eastern China. *Earth and Planetary Science Letters*, 233(1–2): 103–119, doi: [10.1016/j.epsl.2005.02.019](https://doi.org/10.1016/j.epsl.2005.02.019)
- Wu Fuyuan, Yang Jinhui, Wilde S A, et al. 2005b. Geochronology, petrogenesis and tectonic implications of Jurassic granites in the Liaodong Peninsula, NE China. *Chemical Geology*, 221(1–2): 127–156, doi: [10.1016/j.chemgeo.2005.04.010](https://doi.org/10.1016/j.chemgeo.2005.04.010)
- Xie Chaoming, Li Cai, Wang Ming, et al. 2014. Tectonic affinity of the Nyainrong microcontinent: constraints from zircon U-Pb age and Hf isotopes compositions. *Geological Bulletin of China (in Chinese)*, 33(11): 1778–1792
- Xiu Chun, Zhang Daojun, Zhai Shikui, et al. 2016. Zircon U-Pb age of granitic rocks from the basement beneath the Shi Island, Xisha Islands and its geological significance. *Marine Geology & Quaternary Geology (in Chinese)*, 36(3): 115–126
- Xu Xisheng. 2008. Several problems worthy to be noticed in the research of granites and volcanic rocks in SE China. *Geological Journal of China Universities (in Chinese)*, 14(3): 283–294
- Xu Wangchun, Zhang Hongfu, Liu Xiaoming. 2007. U-Pb zircon dating constraints on formation time of Qilian high-grade metamorphic rock and its tectonic implications. *Chinese Science Bulletin*, 52(4): 531–538, doi: [10.1007/s11434-007-0082-7](https://doi.org/10.1007/s11434-007-0082-7)
- Xu Changhai, Zhang Lu, Shi Hesheng, et al. 2017. Tracing an Early Jurassic magmatic arc from South to East China Seas. *Tectonics*, 36(3): 466–492, doi: [10.1002/2016TC004446](https://doi.org/10.1002/2016TC004446)
- Yan Quanshu, Castillo P, Shi Xuefa, et al. 2015. Geochemistry and petrogenesis of volcanic rocks from Daimao Seamount (South China Sea) and their tectonic implications. *Lithos*, 218–219: 117–126, doi: [10.1016/j.lithos.2014.12.023](https://doi.org/10.1016/j.lithos.2014.12.023)
- Yan Quanshu, Shi Xuefa. 2009. Characteristics of volcanoclastic rocks from seamounts in the South China Sea and its geological implications. *Acta Petrologica Sinica (in Chinese)*, 25(12): 3327–3334
- Yan Quanshu, Shi Xuefa, Castillo P R. 2014. The late Mesozoic-Cenozoic tectonic evolution of the South China Sea: a petrologic perspective. *Journal of Asian Earth Sciences*, 85: 178–201, doi: [10.1016/j.jseaes.2014.02.005](https://doi.org/10.1016/j.jseaes.2014.02.005)
- Yan Quanshu, Shi Xuefa, Liu Jihua, et al. 2010. Petrology and geochemistry of Mesozoic granitic rocks from the Nansha micro-block, the South China Sea: constraints on the basement nature. *Journal of Asian Earth Sciences*, 37(2): 130–139, doi: [10.1016/j.jseaes.2009.08.001](https://doi.org/10.1016/j.jseaes.2009.08.001)
- Yan Quanshu, Shi Xuefa, Wang Kunshan, et al. 2008a. LA-ICPMS zircon U-Pb dating of granitic rocks from the Nansha micro-block, South China Sea, and its geological significance. *Acta Geologica Sinica (in Chinese)*, 82(8): 1057–1067
- Yan Quanshu, Shi Xuefa, Wang Kunshan, et al. 2008b. Major element, trace element, and Sr, Nd and Pb isotope studies of Cenozoic basalts from the South China Sea. *Science in China Series D: Earth Sciences*, 51(4): 550–566, doi: [10.1007/s11430-008-0026-3](https://doi.org/10.1007/s11430-008-0026-3)
- Yan Quanshu, Shi Xuefa, Yang Yaomin, et al. 2008c. Potassium-argon/argon-40-argon-39 geochronology of Cenozoic alkali basalts from the South China Sea. *Acta Oceanologica Sinica*, 27(6): 115–123
- Yang Shuying, Fang Nianqiao. 2015. Geochemical variation of volcanic rocks from the South China Sea and neighboring land: implication for magmatic process and mantle structure. *Acta Oceanologica Sinica*, 34(12): 112–124, doi: [10.1007/s13131-015-0759-8](https://doi.org/10.1007/s13131-015-0759-8)
- Yao Bochu, Wan Ling. 2006. *The Three-Dimensional Structure of Lithosphere and its Evolution in the South China Sea (in Chinese)*. Beijing: Geology Press, 113–116
- Yao Bochu, Wan Ling, Wu Nengyou. 2004. Cenozoic plate tectonic activities in the Great South China Sea area. *Geology in China (in Chinese)*, 31(2): 113–122
- Yuan Xiaobo, Fang Nianqiao, Zhang Zhenguo, et al. 2019. The characteristics of granites in the Gaofeng and Baocheng areas, Hainan Province, China: response to subduction of the Tethyan South China Sea. *Geologia Croatica*, 72(Special issue): 93–109, doi: [10.4154/gc.2019.19](https://doi.org/10.4154/gc.2019.19)
- Yuan Wei, Yang Zhenyu, Zhao Xixi, et al. 2018. Early Jurassic granitoids from deep drill holes in the East China Sea Basin: implications for the initiation of Palaeo-Pacific tectono-magmatic cycle. *International Geology Review*, 60(7): 813–824, doi: [10.1080/00206814.2017.1351312](https://doi.org/10.1080/00206814.2017.1351312)
- Yue Junpei, Zhang Yan, Shen Huailei, et al. 2013. Constraints of geological characteristics of the South China continental margin on the basement of basins in northern South China Sea. *Acta Petrologica Sinica (in Chinese)*, 34(S2): 120–128
- Zhang Hongfei, Jin Lanlan, Li Zhang, et al. 2007. Geochemical and Pb-Sr-Nd isotopic compositions of granitoids from western Qinling belt: constraints on basement nature and tectonic affinity. *Science in China Series D: Earth Sciences*, 50(2): 184–196, doi: [10.1007/s11430-007-2015-3](https://doi.org/10.1007/s11430-007-2015-3)
- Zhang Cuimei, Manatschal M, Pang Xiong, et al. 2020c. Discovery of mega-sheath folds flooring the Liwan subbasin (South China Sea): implications for the rheology of hyperextended crust. *Geochemistry, Geophysics, Geosystems*, 21(7): e2020GC009023, doi: [10.1029/2020GC009023](https://doi.org/10.1029/2020GC009023)
- Zhang Qiao, Wu Shiguo, Dong Dongdong. 2016. Cenozoic magmatism in the northern continental margin of the South China Sea: evidence from seismic profiles. *Marine Geophysical Research*, 37(2): 71–94, doi: [10.1007/s11001-016-9266-3](https://doi.org/10.1007/s11001-016-9266-3)
- Zhang Qiao, Wu Shiguo, Lv Fuliang, et al. 2014. The seismic characteristics and the distribution of the igneous rocks in the northwest slope of the South China Sea. *Geotectonica et Metallogenia (in Chinese)*, 38(4): 919–938
- Zhang Yu, Yu Kefu, Fan Tianlai, et al. 2020a. Geochemistry and petrogenesis of Quaternary basalts from Weizhou Island, northwestern South China Sea: evidence for the Hainan plume. *Lithos*, 362–363: 105493, doi: [10.1016/j.lithos.2020.105493](https://doi.org/10.1016/j.lithos.2020.105493)
- Zhang Yu, Yu Kefu, Qian Handong. 2018. LA-ICP-MS analysis of

- clinopyroxenes in basaltic pyroclastic rocks from the Xisha Islands, northwestern South China Sea. *Minerals*, 8(12): 575, doi: [10.3390/min8120575](https://doi.org/10.3390/min8120575)
- Zhang Yu, Yu Kefu, Qian Handong, et al. 2020b. The basement and volcanic activities of the Xisha Islands: evidence from the kilometre-scale drilling in the northwestern South China Sea. *Geological Journal*, 55(1): 571–583, doi: [10.1002/gj.3416](https://doi.org/10.1002/gj.3416)
- Zhao Guochun, Zhai Mingguo. 2013. Lithotectonic elements of Precambrian basement in the North China Craton: review and tectonic implications. *Gondwana Research*, 23(4): 1207–1240, doi: [10.1016/j.gr.2012.08.016](https://doi.org/10.1016/j.gr.2012.08.016)
- Zheng Jianping, Griffin W L, O'Reilly S Y, et al. 2006. Widespread Archean basement beneath the Yangtze craton. *Geology*, 34(6): 417–420, doi: [10.1130/G22282.1](https://doi.org/10.1130/G22282.1)
- Zhou Xinmin, Li Wuxian. 2000. Origin of Late Mesozoic igneous rocks in Southeastern China: implications for lithosphere subduction and underplating of mafic magmas. *Tectonophysics*, 326(3-4): 269–287, doi: [10.1016/S0040-1951\(00\)00120-7](https://doi.org/10.1016/S0040-1951(00)00120-7)
- Zhou Jian, Liu Bo, Shao Mingli, et al. 2022. Lithologic classification of pyroclastic rocks: a case study for the third member of the Hushiling Formation, Dehui fault depression, Songliao Basin, NE China. *Journal of Petroleum Science and Engineering*, 214: 110456, doi: [10.1016/j.petrol.2022.110456](https://doi.org/10.1016/j.petrol.2022.110456)
- Zhu Weilin, Xie Xinong, Wang Zhenfeng, et al. 2017. New insights on the origin of the basement of the Xisha Uplift, South China Sea. *Science China Earth Sciences*, 60(12): 2214–2222, doi: [10.1007/s11430-017-9089-9](https://doi.org/10.1007/s11430-017-9089-9)
- Zhu Jingjing, Zhong Hong, Xie Guiqing, et al. 2016. Origin and geological implication of the inherited zircon from felsic dykes, Youjiang basin, China. *Acta Petrologica Sinica* (in Chinese), 32(11): 3269–3280